Available online at www.sciencedirect.com
SCIENCE DIRECT®

Journal of the European Ceramic Society 23 (2003) 1715–1722
www.elsevier.com/locate/jeurceramsoc

Actual relationship between load and deflection for cellular ceramic substrates: effective moduli of substrates and materials

V. Shustorovich, E. Shustorovich*

American Scientific Materials Technologies (ASMT) Co, 485 Madison Avenue, 24th Floor, New York, NY 10022, USA

Received 1 May 2002; received in revised form 23 October 2002; accepted 2 November 2002

Abstract

Many practically important ceramic materials show inelastic behavior well beyond the elastic limit. However, because the appropriate load-deflection (stress–strain) diagrams are usually unavailable, particularly for thin-walled substrates, the elastic (Young's) moduli, **E**, are commonly used for estimating mechanical and thermal stresses. We have developed an experimental device to directly measure deflection of outer layers of round cellular ceramic substrates under uniform radial pressure, which allowed us to obtain the complete load-deflection diagram up to the crush point, providing the ultimate (crush) strength of the ceramic substrates and eventually the ultimate (wall) strength of substrate materials. The materials were ASMT hematite Fe_2O_3 and titania TiO_2 (as well as common cordierite), and the substrates had both closed and open cell designs with straight and skewed channels. We found that at all applied loads the substrate deflections were inelastic. However, in all diagrams a basic part was found to be nearly linear providing for the radial modulus, which we defined as the *effective modulus of the substrate*, $\boldsymbol{E_q}$*****. On this basis, we have determined the *effective modulus of the substrate material*, $\mathbf{E_q}$. We found $\mathbf{E_q}$ to be much smaller than **E**, typically by an order of magnitude or more. Advantages of using $\mathbf{E_q}$ instead of **E** are discussed. We also argue that evaluation of the allowable pressure on a substrate should be based on the ultimate pressure corrected by the safety/load factor, **k**, whose estimates are discussed.

Keywords: Cellular structures; Fe_2O_3; Mechanical properties; Strength; Substrates; Testing; TiO_2

1. Introduction

Automotive catalytic converters widely employ cellular ceramic substrates, typically made from cordierite, $2MgO{\cdot}2Al_2O_3{\cdot}5SiO_2$, and sometimes from other metal oxides. To enhance performance, the substrates are made with a higher cell density and thinner walls but this leads to the decreased mechanical strength. Rational optimization of these opposite trends requires knowledge of the load-deflection (stress–strain) diagrams, which for most ceramic materials are not available, particularly for thin-walled substrates. For this reason, the elastic (Young's) moduli, **E**, are commonly used for estimating mechanical and thermal stresses in all ceramic substrates, including thin-walled ones.[1]

There are two fundamental problems with this practice. The first one relates to the efficiency of the elastic approximation for working loading regimes of ceramic materials, particularly for evaluating the ultimate strain and strength. The second problem concerns with specifics of thin-wall ceramic structures. We will briefly comment on both problems.

Evaluation of strength based on the concept of the elastic modulus is justified only for brittle materials (such as glass) for which plastic deformation is very small and failure occurs just after the elastic limit is reached.[2–4] However, this is not the case for many ceramic materials, including cordierite, which show deformation without failure well beyond the elastic limit. For such materials, termed as "relatively brittle" by Gogotsi, [5] the actual stress–strain diagram with the ultimate strain, being much bigger than the elastic one, is arguably more informative for evaluating thermal shock resistance and other characteristics. [5] However, because such diagrams usually are not available, it is

* Corresponding author. Tel.: +1-585-383-8768; fax: +1-240-414-4561.

E-mail address: eshusto1@rochester.rr.com (E. Shustorovich).

0955-2219/02/$ - see front matter
PII: S0955-2219(02)00399-0

still a common practice to use the elastic moduli, **E**, for evaluating various properties of all ceramic materials, and efforts continue to be focused on developing and refining techniques of obtaining the values of **E**. [6]

The value of **E** is commonly determined by acoustical methods measuring natural frequencies of uniform bulk samples, having shapes of small beams, rectangular bars, discs, etc. [1,6] It is not clear how to make such samples representative of cellular ceramic structures having non-uniform thickness (e.g. very thin inner walls and a much thicker outer skin) and geometries, which are much different in axial vs. in-plane directions. For example, for cylindrical honeycomb substrates an acoustic test has been suggested to estimate the elastic modulus of the whole monolithic structure but only in the axial direction.[1] But such a test is not informative for evaluating the in-plane modulus, which is of major practical interest.

Similarly, known methods of determining material mechanical properties, such as tensile (bending) strength and crack resistance, which employ beam-like samples undergoing the three- (or four-) point bending test, [1,5] cannot be applied to cellular thin-walled ceramic materials. Cell walls have the thickness of tens or (at most) hundreds of microns, while the tested bulk samples have to be thicker by two orders of magnitude. Therefore, in order to estimate the material strength obtained from the bulk samples for thin-walled cellular structures one has to use Weibull's statistics, [1] when the empirical nature of many parameters (often not well-defined) makes quantitative estimates uncertain.

In common practice, the experimental strength of cylindrical ceramic cellular substrates, particularly cordierite ones, is determined indirectly, usually by measuring the substrate's isostatic crush strength and then theoretically re-scaling it for the actual case of uniform radial pressure on the lateral surface of the substrate. [7] However, this approach has fundamental difficulties. First, its analytical formalism assumes elastic deformation of a solid structure. As said above, for substrate materials such as cordierite the elastic approximation employing constants such as the elastic modulus may be grossly inadequate. Second, whatever value of the ultimate strength has been obtained, this gives only the load (stress) without knowing the deflection (strain). Thus, this or other similar tests, measuring only the crush strength, provide no information on load-deflection relationship in ceramic materials and substrates.

American Scientific Materials Technologies (ASMT) has developed a proprietary process of making metal oxide (ceramic) products by direct oxidation of appropriate metallic preforms, retaining their shape in the process. [8, 9] Thus, a big variety of metallic preforms can be reproduced in ceramics. The best studied metals were iron and titanium forming hematite Fe_2O_3 and titania (rutile) TiO_2 products, respectively. In particular, for the first time this allowed one to make ceramic substrates with unique designs known only for metallic substrates, both with closed and open cells. One such design employs spirally wound, alternating flat (1) and corrugated (2) layers that produces substrates with straight (parallel) channels and closed cells of quasi-triangular shape, as shown in Fig. 1. For all details of this and other designs the reader is referred to ref. [8] The new materials and new designs required new informative testing.

Accordingly, we have developed an experimental device imitating pressure conditions in canned substrates. Specifically, we have directly measured deflection of outer layers of cylindrical cellular ceramic substrates under uniform radial pressure, which allowed us to obtain a complete load-deflection diagram up to the crush point. The ceramic materials were the ASMT hematite and titania, and the substrates, having a wide range of cell density, included designs with both closed and open cells of varied wall thickness. Below we will report testing results for substrates with closed quasi-triangular cells, as illustrated in Fig. 1. For comparison, a conventional round cordierite substrate with closed square cells was similarly tested. From the load-deflection diagram, we were able to estimate the effective radial modulus of the substrate, $\mathbf{E_q}$*. On this experimental basis, combined with theoretical modeling of stress distribution in all layers of a substrate of a given geometry, [8] we have determined the ultimate (wall) strength and the effective modulus of the substrate material, $\mathbf{E_q}$.

The paper will be organized as follows. First, we will describe the essence of the experimental device and procedures followed by experimental findings. Then, we will explain how the values of $\mathbf{E_q}$* were obtained and provide a theoretical formalism to interrelate $\mathbf{E_q}$* and $\mathbf{E_q}$. Finally, we will comment on the necessity of determining the actual load-deflection diagram for ceramic substrates, particularly thin-walled, loaded beyond the elasticity limit. Advantages of using the effective parameters, $\mathbf{E_q}$* and $\mathbf{E_q}$, and theoretical grounds for evaluating the safety/load factor will be discussed.

2. Experimental device and tested substrates

The load-deflection diagrams were obtained at room temperature for the round thin-walled ASMT hematite and titania substrates having closed quasi-triangular cells with straight channels. Geometrical parameters of the tested samples are shown in Table 1. For the sake of comparison, a round 400/6.5 cordierite substrate with closed square cells and straight channels was similarly tested.

The experimental device was designed to determine strength related features of cylindrical thin-walled honeycomb substrates by applying external uniform radial pressure (URP) to a lateral round surface of the sample.

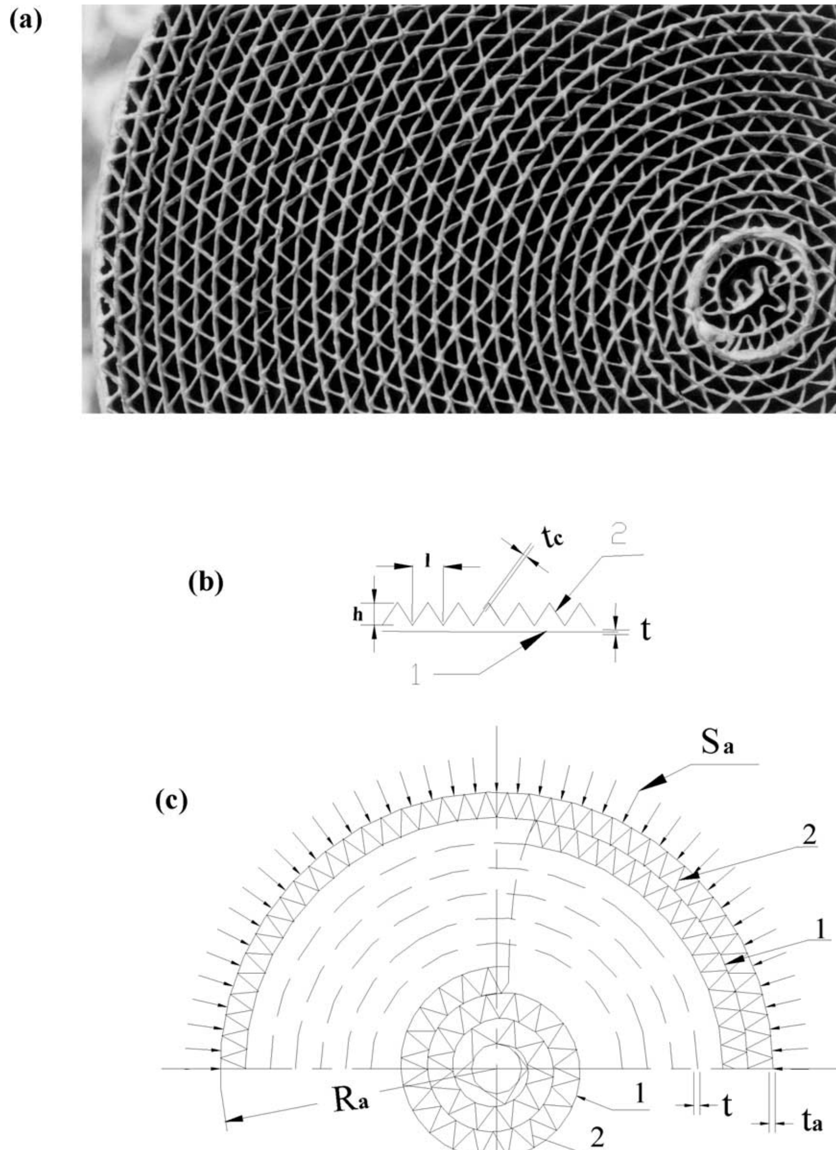

Fig. 1. ASMT ceramic structure with straight parallel channels and closed quasi-triangular cells: (a) photograph of part of the structure; (b) schematics of the alternating flat (1) and corrugated (2) layers; (c) schematics of the ceramic structure retaining shape of a metallic preform made by spiral winding of alternating flat (1) and corrugated (2) layers. See text for notations.

Table 1
Geometric parameters of ASMT closed cell hematite and titania substrates[a]

Sample parameters										
Type	Material	ν	R_a(mm)	H(mm)	N(cpsc)	l(mm)	h(mm)	t_a(mm)	t(mm)	t_c(mm)
I	Hem	0.33	45.0	76.2	132	1.70	0.90	0.40	0.09	0.06
II	Hem	0.33	45.0	76.2	132	1.70	0.90	0.40	0.12	0.06
III	Tit	0.28	45.0	76.2	132	1.70	0.90	0.60	0.10	0.05
IV	Tit	0.28	45.0	76.2	54	2.74	1.37	0.50	0.10	0.10

[a] Notations: Hem (hematite), Tit (titania), ν (Poisson's ratio taken from Ref. [11]). See Fig. 1b and text for other notations.

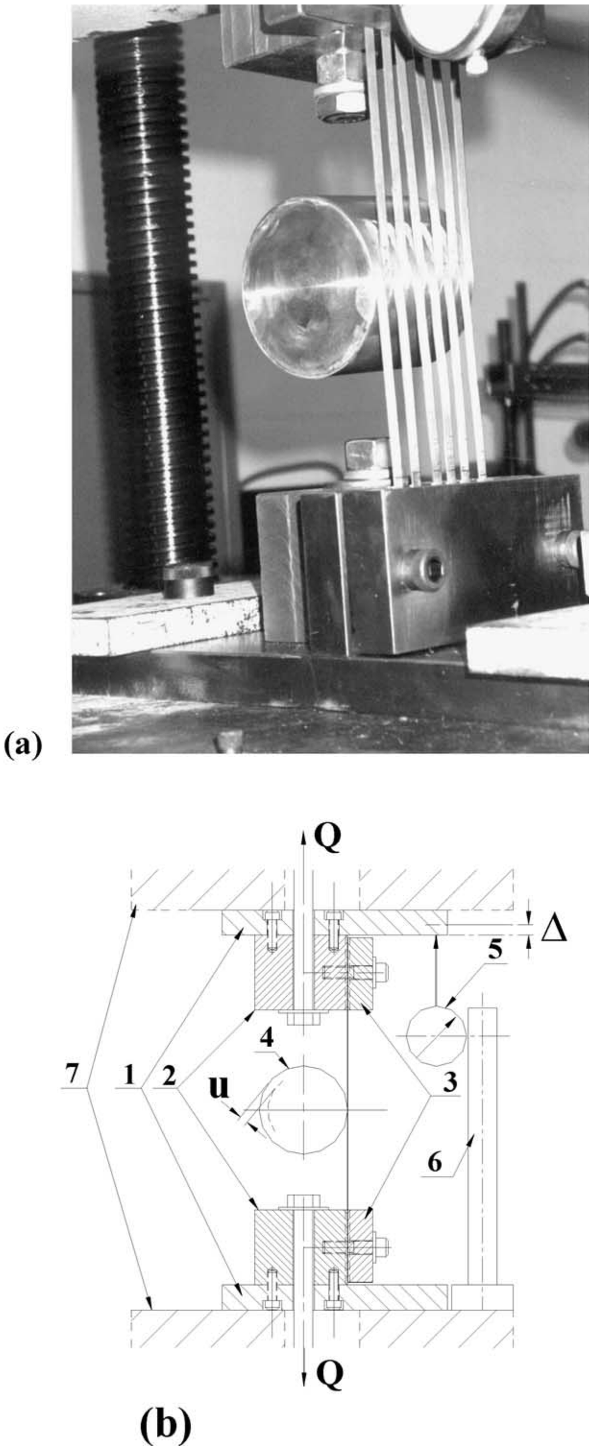

Fig. 2. Experimental device for testing round substrates under uniform radial pressure: photograph (a) and schematics (b) of the device. Fig. 2a also demonstrates the working position of a tested substrate. See text for notations.

A photograph of the device with a tested substrate is shown in Fig. 2a. The device's schematics are shown in Fig. 2b. The device includes two base plates ***1*** with guides ***2*** and clamps ***3***. Vertical loads Q from a testing machine are transformed into URP $\boldsymbol{S_a}$ (cf. Fig. 1c) on

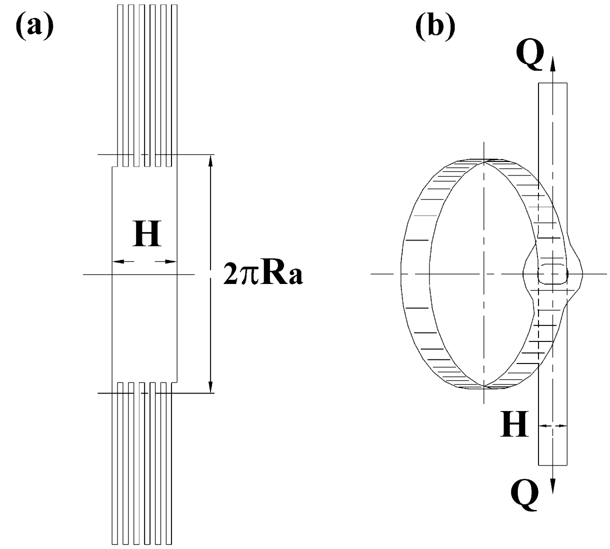

Fig. 3. Steel bands used in the testing: (a) schematic of a band with stripes on the ends (this band, enveloping a tested substrate, is also shown in Fig. 2a); (b) schematic of a belt-buckle band (in a working position).

the sample by using a specially designed band ***4*** made of stainless steel. The band, tightly enveloping the round sample's surface, had its opposite ends firmly fixed between the guides and clamps, so that when load was applied, the band uniformly squeezed the substrate and made it contracted in the radial direction. Two band types were used: a band with stripes on the ends and a belt-buckle band, whose schematics are shown in Fig. 3a and 3b, respectively (see also Fig. 2a). A precision micron dial indicator ***5*** with a stand ***6*** was used to measure an effective increase, Δ, in the distance between the upper and bottom cross-rails *7*, which (after subtracting the intrinsic band lengthening) determines a radial deflection, **u**, of the sample as a function of $\boldsymbol{Q}$ and the corresponding value of S_a. Loading was discreet with equal intervals of $\boldsymbol{Q}$ until the sample was crushed. As a result, the load–deflection diagram was obtained including the ultimate load $\boldsymbol{Q_m}$ and crush strength of the sample $\boldsymbol{S_{am}}$ (ultimate URP).

For a cylindrical substrate, where $\mathbf{R_a}$ and **H** are its outer radius and height, the load **Q** to create URP $\boldsymbol{S_a}$ is

$$Q = S_a\, R_a\, H, \tag{1}$$

hence

$$S_a = Q/(\, R_a\, H). \tag{2}$$

The radial deflection of a lateral surface of the sample is

$$u = \Delta/(2\pi), \tag{3}$$

where Δ is a linear deflection (see above).

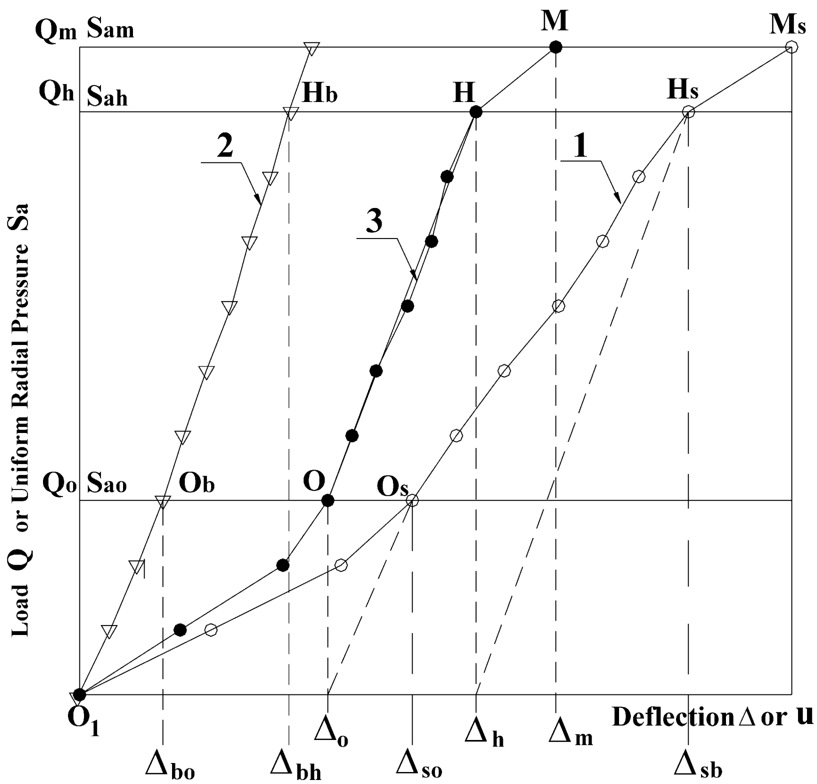

Fig. 4. Typical load-deflection diagram for round ceramic substrates under uniform radial pressure. Shown are three graphs: (1) the substrate and band; (2) the band only; (3) the substrate only. The tested samples were ASMT hematite and titania substrates (with both closed and open cells) and conventional cordierite substrate. See text for notations and explanations.

3. Results and discussion

3.1. Load–deflection diagram

Fig. 4 illustrates a typical load–deflection diagram for the mentioned ceramic substrates. The coordinate axes correspond to loads **Q** (or pressure $\boldsymbol{S_a}$) and deflection (linear Δ or radial u). Each diagram consists of three graphs. Graph 1 shows the combined **Q** ($\boldsymbol{S_a}$) vs Δ (u) diagram for the sample and band, Graph 2 for the band only, and Graph 3 for the sample only (obtained by subtracting the values of Δ or **u** of Graph 2 from those of Graph 1).

The mean experimental values of **Q** ($\boldsymbol{S_a}$) and Δ (**u**) are summarized in Table 2. The load range, within which no apparent failure occurred, typically was $\boldsymbol{Q_o}$ ≈2000 N (450 lb) to Q_h ≈4500 N (1000 lb) corresponding to radial pressure $\boldsymbol{S_{ao}}$ ≈0.5 MPa (70 psi) to $\boldsymbol{S_{ah}}$ ≈1.2 MPa (175 psi). The crush strength was within the pressure range of S_{am} ≈1.1–2.1 MPa (150–300 psi). The deflection range was up to Δ ≈1 mm.

Measurements began after the initial pressure $\boldsymbol{S_{ao}}$ was large enough, typically, above 0.5 MPa, to make the band tightly wound around the sample to cause radial contraction (point O). For all substrates, in Graphs 3 (and 1) one could distinguish three parts. The first one, denoted as O_1O, corresponds to loads that eliminate various gaps in the load system. This part is non-linear and has a relatively small effective slope versus the deflection axis. The second, basic part of the diagram, denoted as OH, corresponds to loads that cause radial

Table 2
Mean effective moduli for ASMT substrates, $\boldsymbol{E_q}$*, and materials, $\boldsymbol{E_q}$

Sample		Parameters[b]									
Type[a]	Amount	Q_o(N)	S_{ao} (MPa)	Δ_o(mm)	Q_h(N)	S_{ah}(MPa)	Δ_h(mm)	$\boldsymbol{E_q}$*(GPa)	$\boldsymbol{S}$*–	$\boldsymbol{E_q}$(GPa)	S_{am}(MPa)
I	12	1780	0.52	0.36	4005	1.17	0.58	0.56	11.8	6.66	1.66
II	12	2781	0.81	0.49	4561	1.33	0.64	0.66	10.8	7.10	1.72
III	6	2225	0.65	0.50	4895	1.43	0.76	0.60	12.5	7.52	2.10
IV	3	2002	0.58	0.21	3338	0.97	0.36	0.53	14.8	7.86	1.05

[a] See Table 1.
[b] See Fig. 4 and text for notations.

deformation of the substrate's round surface without any apparent failure. In all diagrams, the second part was found to be nearly linear, with a larger slope. The third, final part, denoted as HM, corresponds to developing failure of the substrate outermost layers and, similar to the first part, O_1O, has a smaller slope.

At all steps, after unloading we always observed some irreversible deformation, which is illustrated by inclined dashed lines on Graph 1 (substrate and band), with slopes close to those on Graph 2 (band only). When load was applied again, deflection began only at the larger load. For simplicity, the dashed lines on Graph 3 (substrate only) are shown as vertical, although they are somewhat inclined and have very small loops between loading and unloading lines. This kind of inelastic behavior beyond the elastic limit for ductile materials is well known as plastic flow with work-hardening. [10] However, in the studied ceramic materials all OH parts of the diagrams have been obtained beyond the elastic limit; so, even if some elasticity region existed, it was very small and we didn't observe it.

We have similarly tested a common cordierite 400/6.5 substrate with square 1.27 mm cells [cell density 62 cpsc (400 cpsi), wall thickness 0.16 mm (6.5 mils)]. The substrate's size was $R_a = 45.0$ mm and $H = 76.2$ mm. Qualitatively, the stress–strain diagram was the same as those shown in Fig. 4 for the ASMT hematite and titania.

Fig. 4 clearly shows that for the studied thin-walled substrates the relationship between load and radial deflection for working loads preceding failure is effectively described by the nearly linear part OH. This linear part was used to estimate the effective radial modulus (taking into account inelastic effects), which we defined as the effective modulus of the substrate, $\boldsymbol{E_q}$*.

Because $\boldsymbol{E_q}$* is the slope of the load–deflection (stress–strain) diagram in the linear plastic region, it can be considered as an analog of the strengthening modulus of a ductile material. [10] The major difference is that $\boldsymbol{E_q}$* characterizes ceramic materials having practically no elastic region.

3.2. *Evaluation of effective modulus of the substrate material,* $\mathbf{E_q}$

Now we turn to determining the effective modulus of the substrate material, $\boldsymbol{E_q}$.

In the quasi-elastic approximation, for an ASMT closed cell substrate considered as a solid cylinder under uniform radial pressure $\boldsymbol{S_{à}}$ on its lateral surface (Fig. 1b), the radial deflection will be

$$\boldsymbol{u} = (1-\nu) \times \boldsymbol{R_a} \left(\boldsymbol{S_a} / \boldsymbol{E_q}^*\right), \tag{4}$$

hence

$$\boldsymbol{E_q}^* = (\boldsymbol{1}-\nu) \times \boldsymbol{R_a} \, (\boldsymbol{S_a}/\boldsymbol{u}) \tag{5}$$

where $\boldsymbol{\nu}$ is Poisson's ratio. From Eqs. (2) and (3), in terms of $\mathbf{Q}$ and $\boldsymbol{\Delta}$, one gets

$$\boldsymbol{Eq}^* = (1-\nu) \times (2\pi/\boldsymbol{H}) \times (\boldsymbol{Q}/\Delta) \tag{6}$$

Using notations, explained above and used in Fig. 4, one gets

$$\boldsymbol{E}_{\mathrm{q}}^* = (1-\nu) \times \boldsymbol{R}_a(\boldsymbol{S}_{\mathrm{ah}} - \boldsymbol{S}_{\mathrm{ao}})/(\boldsymbol{u}_{\mathrm{h}} - \boldsymbol{u}_o) \tag{7}$$

or

$$\boldsymbol{E}_{\mathrm{q}}^* = (1-\nu) \times (2\pi/\boldsymbol{H}) \times \left(\boldsymbol{Q}_{\mathrm{h}} - \boldsymbol{Q}_{\mathrm{o}}\right)/(\Delta_{\mathrm{h}} - \Delta_{\mathrm{o}}), \tag{8}$$

where

$$\Delta_{\mathrm{h}} = \Delta_{\mathrm{sh}} - \Delta_{\mathrm{bh}} \tag{9}$$

and

$$\Delta_{\mathrm{o}} = \Delta_{\mathrm{so}} - \Delta_{\mathrm{bo}} \tag{10}$$

If one knows the circumferential stress $\boldsymbol{S_{ta}}$ in the outer round flat layer (see the relevant formalism in Ref. [8]), the deflection in Eq. (4) can be expressed as

$$\boldsymbol{u} = \boldsymbol{S}_{\mathrm{ta}}\boldsymbol{R}_{\mathrm{a}}/\left[\boldsymbol{E}_{\mathrm{q}}/(1-\nu)\right] \tag{11}$$

where $\boldsymbol{E_q}$ is the effective modulus of the substrate material.

From Eqs. (4) and (11) we get

$$\boldsymbol{E}_{\mathrm{q}} = \boldsymbol{E}_{\mathrm{q}}^*\boldsymbol{S}^* \tag{12}$$

Thus, in order to interrelate $\boldsymbol{E_q}$ and $\boldsymbol{E_q}$* one should know $\boldsymbol{S}$*.

For the considered ASMT closed cell substrate (Fig. 1), from Eqs. (4), (11) and (12) we have

$$\boldsymbol{S}^* = \boldsymbol{S}_{\mathrm{ta}}/\boldsymbol{S}_{\mathrm{a}} \tag{13}$$

Eq. (12), interrelating $\boldsymbol{E_q}$ and $\boldsymbol{E_q}$*, is general and valid for other designs, for which the appropriate values of $\boldsymbol{S}$* should be determined.[8]

For the considered closed cell cordierite substrate, the well known relationship is [1]

$$\boldsymbol{S}^* = \boldsymbol{h}/\boldsymbol{t} \tag{14}$$

Thus, having obtained experimentally the relation between $\boldsymbol{S_a}$ and $\boldsymbol{u}$ or $\boldsymbol{Q}$ and Δ, one can determine $\boldsymbol{E_q}$* [see Eqs. (7) or (8)] and then, having calculated $\boldsymbol{S}$* (as shown above), one can determine $\boldsymbol{E_q}$. Similarly, one can determine the ultimate (wall) strength of the substrate material by using the experimental crush strength of substrate, $\boldsymbol{S_{am}}$, and the calculated value of the maximum wall stress. [8]

Table 1 gives parameters of the tested closed cell substrates. There were four types of them, differing by materials (hematite and titania), geometries (radius, height, cell density and cell size), and the cell wall thickness. Table 2 provides, for each substrate type, the mean values of relevant characteristics, including the load-deflection measurements (applied pressures and deflections) within the linear range OH, the crush strength, and the moduli $\mathbf{E}_q$* and $\mathbf{E}_q$.

Despite significant differences in the substrate geometry, the values of $\mathbf{E_q}$, characteristic of the material, proved to be very close, which argues for the reasonability of modeling. For example, for titania substrates of types III and IV, differing in cell density by a factor of almost three, the material moduli $\mathbf{E_q}$ (7.52 vs. 7.86 GPa) are very close. As seen from Table 2, the mean values of the effective moduli of ASMT materials are $\mathbf{E_q} = 6.9 \pm 0.2$ GPa (1×10^6 psi) for hematite and $\mathbf{E_q} = 7.7 \pm 0.2$ GPa (1.1×10^6 psi) for titania.

We have also obtained the load-deflection diagrams for ASMT hematite substrates with a totally different design having open cells and skewed channels (described in detail in [8]). Because the diagrams were very similar to those in Fig. 4 for the closed cell design, we won't reproduce them here. Most importantly, although the effective substrate moduli $\mathbf{E_q}$* were very different (as should be), the effective modulus $\mathbf{E_q}$ of the material was found to be rather insensitive to the design (closed or open cell), which is indicative of the reasonability of theoretical modeling.

We found $\mathbf{E_q}$ to be much smaller than the elastic (Young's) modulus, E. For example, for tetragonal titania (rutile) TiO_2, the cited value of **E** is 283 GPa (41×10^6 psi),[11] which is 40 times larger. The similar (but less dramatic) difference was found for cordierite. From our testing (see above), we found the cordierite effective modulus to be $\mathbf{E}_q = 9.7$ GPa (1.4×10^6 psi), which is 2–3 times smaller than the literature values of $\mathbf{E} \approx 19.3$–26.2 GPA (2.8–3.8×10^6 psi).[7,8]

3.3. Safety/load factor and patterns of failure

Fig. 4 also provides theoretical and methodological grounds for choosing a safety/load factor, **k**, from the crush strength, $\mathbf{S_{am}}$ ($\mathbf{Q_m}$). The minimal safety/load factor, $\mathbf{k_m}$, can be estimated as the ratio

$$\boldsymbol{k}_{\mathrm{m}} = \boldsymbol{S}_{\mathrm{am}}/\boldsymbol{S}_{\mathrm{ah}} = \boldsymbol{Q}_m/\boldsymbol{Q}_{\mathrm{h}} \qquad (15)$$

where the value of $\boldsymbol{S}_{\mathbf{ah}}$ ($\boldsymbol{Q}_{\mathbf{h}}$) corresponds to the onset of substrate's failure. For hematite substrates, we found $\mathbf{k_m} = 1.29$–1.42. Of course the practical safety factor, **k**, should be larger, $\mathbf{k} > \mathbf{k_m}$ (more specific numerical estimates of **k** require to take into account various working loads on substrates and more experimental data for a statistical analysis). For comparison, evaluating the strength of round honeycomb substrates is commonly made within the isostatic pressure approach. [7] Here the allowable canning pressure relates to the isostatic ultimate (crush) strength (theoretically re-scaled to the maximal uniform radial pressure), the former being taken to be smaller by an order of magnitude than the latter.[7] Such a safety/load factor seems to be excessive but the approach doesn't provide any ground for correlating the critical value of the substrate's strength with the allowable canning pressure.

The original concept of the elastic modulus is still utilized for various complex cases and honeycomb structures. [1, 12] However, when the ultimate load greatly exceeds loads within the elastic range, there is a big load-carrying capacity beyond the elastic limit, and this capacity should be included in design considerations. For such ceramic materials, evaluation of the allowable pressure on a substrate should be based on the ultimate pressure reduced by the safety/load factor (the plastic design method) rather than on stresses within the elastic limit (the elastic design method). [2, 3]

The studied ASMT thin-walled substrates, having designs novel for honeycomb ceramics, showed specific patterns of failure. The failure process, reflected in the HM part of the load-deflection diagram, starts in the outermost layers and continues up to the substrate's collapse (point M), determined by some critical amount of failed elements (fractured meshes) of the structure. Such failure patterns may be analyzed by methods of fracture mechanics. In particular, the values of $\mathbf{S_{ah}}$ (beginning of the substrate's failure) may characterize some threshold stress-intensity factor, and the values of $\mathbf{S_{am}}$ (substrate's collapse) a critical stress-intensity factor.

The above findings are important not only for re-evaluating characteristics of mechanical stresses but also of thermal stresses.[8] Arguably, the thermal shock resistance should be determined by the value of the ultimate strain,[5] which requires knowledge of the complete stress–strain diagram. While evaluating the thermal strength in an inelastic region (where the ultimate strain belongs), one can neglect the much larger elastic (Young's) modulus **E** compared with the effective modulus $\mathbf{E_q}$, because the strength depends on the difference in inverse values of the moduli.[13]

4. Summary and conclusions

We have developed an experimental device, imitating pressure conditions in canned cylindrical cellular thin-walled substrate. The device allows one to directly measure radial deflection of outer layers of substrates under external uniform radial pressure, which reveals the actual relationship between the radial pressure and deflection. We have obtained a complete load-deflection diagram up to a point of failure providing the ultimate (crush) strength of the round ceramic substrates under typical working loading and eventually the ultimate (wall) strength of the substrate materials. The systematically tested substrates were made from ASMT hematite and titania and had closed cells with straight channels. ASMT hematite substrates with open cells and skewed channels as well as a conventional round cordierite substrate with square cells were also tested and analyzed in a similar way.

At applied loads for all tested thin-walled substrates the elastic region was non-observable and the radial deflection was found to be inelastic. However, in each case the basic part of the diagram was nearly linear and, therefore, could be described as the effective modulus, $\mathbf{E_q}$* of a substrate. By using the quasi-elastic approximation and treating explicitly the substrate's geometry, we have developed a theoretical formalism to determine the effective modulus, $\mathbf{E_q}$, of the above ceramic materials.

We found $\mathbf{E_q}$ to be much smaller than **E** (known in the literature), by an order of magnitude or even more. It appears that the common practice of using the elastic (Young's) modulus, **E**, for evaluating mechanical and thermal strength of ceramic substrates, such as the wall strength and thermal shock resistance, may be grossly inaccurate for materials, which have inelastic deformation behavior well beyond the elastic limit. In such cases, the actual relationship between loads and deflections should be determined and used instead, particularly if there is a part described by the effective modulus, $\mathbf{E_q}$. For such ceramic materials, evaluation of the allowable pressure on a substrate should be based on the ultimate (crush) strength corrected by the safety/load factor, **k**, whose estimates are discussed.

Acknowledgements

The authors thank Professor K. S. Solntsev of the Institute of Physicochemical Problems of Ceramic Materials, Russian Academy of Sciences, for providing the ASMT hematite and titania substrates used in this work.

References

1. Hunt, H. E. M., The mechanical strength of ceramic honeycomb monoliths as determined by simple experiments. *Trans I ChemE*, 1993, **71**(Part A), 257–265.
2. Timoshenko, S., *Strength of Materials, Part II, Advanced Theory and Problems*, 3rd edn. Van Nostrand, New York, 1956 (Chapter 10).
3. Timoshenko, S. P. and Gere, J. M., *Mechanics of Materials*. Brooks/Cole Engineering Division, Litton Educational Publishing, Inc, 1972.
4. Manson, S. S., *Thermal Stress and Low-Cycle Fatigue*. McGraw-Hill, New York, 1966.
5. Gogotsi, G. A., Deformational behaviour of ceramics. *J. Eur. Ceram. Soc.*, 1991, **7**, 87–92.
6. See, for example: (a) Quinn, G. D. & Swab, J. J., Elastic modulus by resonance of rectangular prisms: corrections for edge treatments, *J. Am. Ceram. Soc.*, 2000, **83**, 317–320; (b) Matsumoto, T. et al., Measurements of high-temperature elastic properties of ceramics using a laser ultrasonic method, *J. Am. Ceram. Soc.*, 2001, **84** 1521, and references cited therein.
7. Gulati, S. T. and Chen, D. K. S., Isostatic Strength of Porous Cordierite Ceramic Monolith. *SAE Paper No. 910375* (1991).
8. Shustorovich, E., Shustorovich, V. and Solntsev, K. Monolithic Metal Oxide Thin-Wall Substrates with Closed and Open Cells: Optimal Design by Theoretical Modeling and Experiment, *SAE Paper No. 2001-01-0931* (2001).
9. Solntsev, K. A., Shustorovich, E. and Buslaev, Yu. A., Oxidative constructing of thin-walled ceramics (OCTC). *Doklady Chemistry*, 2001, **378**, 492–499.
10. Boley, B. A. and Weiner, J. H., *Theory of Thermal Stresses*. R. E. Krieger Publishing, Malabar, Florida, 1985.
11. Lackey, W. J., Stinton, D. P., Cerny, G. A., Schaffhauser, A. C. and Fehrenbacher, L. L., Ceramic coatings for advanced heat engines—a review and projection. *Adv. Ceram. Mater.*, 1987, **2**, 24–30.
12. Blake, A., *Practical Stress Analysis in Engineering Design*. Marcel Dekker, New York, 1990.
13. Birger, I. A. and Shorr, B. F., In *Thermal Strength of Machine Elements*, ed. I. A. Birger *et al.* Machinery Publishing, Moscow, 1975 (Chapter 4, in Russian).